ARTICLE

Biodiesel Production from Waste Cooking Oil over Mesoporous SO_4^{2-}/Zr-SBA-15

Ji-long Zhang[a,b], Zhi-jie Lei[b], Xiao-chao Zhang[a], Qi Zhang[a], Qun Yi[c], Rui-feng Li[a]*

a. College of Chemistry and Chemical Engineering, Taiyuan University of Technology, Taiyuan 030024, China
b. College of Mining Engineering, Taiyuan University of Technology, Taiyuan 030024, China
c. Key Laboratory of Coal Science and Technology and Ministry of Education and Shanxi Province, Taiyuan University of Technology, Taiyuan 030024, China

Biodiesel production from waste cooking oils over SO_4^{2-}/Zr-SBA-15 catalyst was successfully carried out and investigated. SO_4^{2-}/Zr-SBA-15 catalyst was prepared by one-step process using anhydrous zirconium nitrate as zirconium resource, and endowed with the strong Lewis acid sites formed by supporting the zirconium species onto the SBA-15 surface. The as-prepared SO_4^{2-}/Zr-SBA-15 showed excellent triglyceride conversion efficiency of 92.3% and fatty acid methyl esters (FAME) yield of 91.7% for the transesterification of waste cooking oil with methanol under the optimized reaction conditions: the methanol/oil molar ratio of 30, the reaction temperature of 160 °C, the reaction time of 12 h and 10wt% of catalyst. It was noticed that the as-prepared SO_4^{2-}/Zr-SBA-15 materials with the higher area surface of mesoporous framework and the surface acidity displayed excellent stability and reusability, maintaining high FAME yield of (74 ± 1)% after seven runs of reaction.

Key words: Biodiesel, Zr-SBA-15, Solid acid catalyst, Transesterification, Waste cooking oil

I. INTRODUCTION

Alternative fuels, developed from renewable feedstocks and environmental-friendly energy, have arisen intense attention [1, 2]. Biodiesel, as 'green fuel', is one of the alternative renewable fuels which include the mono-alkyl esters of fatty acid from various oils, such as the vegetable oils, animal fats or waste lipids [3, 4].

Homogeneous alkaline catalyst are currently the most popularly and widely used catalyst for triglyceride conversion, despite high cost associated with the production of conventional fuels [1, 5]. To avoid the formation of soap by saponification with the alkaline catalyst, homogeneous alkaline catalysts usually need refined oils feedstock with low free fatty acid (FFA) content [2, 6, 7]. Unfortunately, in the process of refining, the lower grade feedstocks with high FFA requires a pre-treatment step, in which the FFA content is decreased by esterification with short chain alcohols [5, 8]. In other words, the alternative sources generally result in the large cost because of the required expensive refined oils and a pre-treatment process to reduce the FFA content of the raw materials [4]. What's more, homogeneous alkaline catalysts need to be neutralized after reaction, leav-

ing the waste liquor composed of the main biodiesel by-product, namely, glycerol [4, 9]. More researches have been carried out to investigate the biodiesel formation through transesterification using heterogeneous catalysts. Chopade *et al.* reviewed various types of heterogeneous solid acids, bases on the production of biodiesel from transesterification of triglycerides, and compared the relative yields and conversions from various catalytic systems [10]. Cordeiro *et al.* described the structure, properties, synthesis and performance of compounds that were catalytic active in both esterification and transesterification reactions [11]. It was found that heterogeneous acid catalysts for the production of biodiesel would be an attractive research focus and provided more evidences that these catalysts continued to evolve as viable alternatives [2, 4, 5]. Acid catalysts could realize both the FFA esterification and triglycerides transesterification reactions in a single step [12, 13], but the catalytic activities of acid catalysts in the above-mentioned reactions are substantially lower than those of alkaline catalysts. With regard to the intrinsic properties of catalysts, it is an effective way to adopt strong solid acids with a high concentration of catalytic sites to modify the acid catalysts, accelerating the efficient reaction of FFA esterification and triglycerides transesterification, consequently.

Zirconia-based material, such as sulfated zirconia and tungstated zirconia [14], has been considered as the

---

*Author to whom correspondence should be addressed. E-mail: rfli@tyut.edu.cn, Tel.: +86-351-6010121, FAX: +86-351-6010121

most industrial promising heterogeneous acid catalysts [15]. The zirconia-based catalysts exhibited rather active sites in numerous acid-driven reactions, including the biodiesel production from both the esterification of fatty acids and the transesterification of triglycerides with methanol [5]. Nevertheless, there exist several setbacks limiting the application of zirconia-based materials for producing the biodiesel from waste cooking oil [14]. The mesostructured silica-based supports could enlarge the surface area of zirconia species to solve the lower stability problem [16, 17], and be better applied to the biodiesel product ion from the transesterification of waste cooking oil [5, 18]. Furthermore, the zirconium species formed onto the silica frameworks achieving both Lewis and Brönsted acid sites [16, 19] with varying acid strengths depending on the synthesis conditions [5]. For instance, Iglesias *et al.* synthesized Zr-SBA-15 material with acid properties using zirconocene dichloride as the metal source, which exhibited the enhanced catalytic activity in the transesterification of waste cooking oil with methanol, developing the zirconium-silicon mesoporous materials as highly acidic solid catalysts for their application in the valuable biodiesel production [5, 18]. Gracia *et al.* firstly reported the synthesis of Zr-SBA-15 material through a direct synthesis method using $ZrONO_3 \cdot xH_2O$ as Zr precursor [20]. Thitsartarn *et al.* reported that sulfated zirconia dispersed on SBA-15 could be recycled and reused for at least five cycles without significant decrease in activity and stability in the transesterification of palm oil [21]. Although the above results indicate that sulfated zirconia can be applied for the transesterification of small molecules, the reported Zr precursors are expensive and the reaction temperature is high.

In this work the biodiesel production was carried out from expired cooking oil over SO_4^{2-}/Zr-SBA-15 mesoporous materials synthesized via one-step facile method with anhydrous zirconium nitrate as the zirconium resources. To better understand the effects of Zr precursor and structure of sulfated zirconia materials as well as the reaction process conditions on their catalytic performances in biodiesel production from expired cooking oils, we present here a systematic investigation on the synthesis, the characterization, the performance evaluation, and the selection of optimum reaction condition for the as-prepared catalysts.

II. EXPERIMENTS

A. Materials and preparation of SO$_4$/Zr-SBA-15

Zirconium nitrate ($Zr(NO_3)_4$, Kermel), Tetraethyl orthosilicate (TEOS, Kermel) and Pluronic P123 (PEO_{20}-PPO_{70}-PEO_{20}, Aldrich) were used as the zirconium source, the silicon precursor and the structure directing agent, respectively. Expired cooking oil and methanol (99%, Kermel) were used as transesterification catalytic assays. All chemicals were of analytical

TABLE I The properties of expired cooking oil.

Property	Analytical method	Value
Density (25 °C)	EN ISO 3675:1999	0.89 g/cm^3
Viscosity (25 °C)	EN ISO 3104:1996	56.04 mm^2/s
Surface tension	GB/T 22237-2008	38.16 N/m
Water content		99 mg/kg
Acid value	EN ISO 660:2000	0.36 mg KOH/g
Iodine value	EN ISO 14111	128.0 g/100g
Saponification	EN ISO 3657:2013	191.43 mg KOH/g

grade. The properties of waste cooking oil are listed in Table I. The components of glycerides are 2.11wt%, 23.74wt%, 73.28wt%, and 0.87wt% for linoleic acid, palmitic acid, oleic acid, and peanut acid, respectively.

SO_4^{2-}/Zr-SBA-15 materials were synthesized via an improved method [17], using $Zr(NO_3)_4$ as zirconium resource. In a typical process, 1.0 g P123 was dissolved in 40 mL (1 mol/L) sulfated acid solution and stirred for 3 h at 40 °C. Then, 2.3 mL TEOS was added in the mixture and stirred for 2 h. After completely dissolving, appropriate $Zr(NO_3)_4$ was added to the above solution to obtain the desired Zr/Si molar ratio and stirred for 5 h at 40 °C. The obtained solution was then transferred into Teflon-lined autoclave, and heated at 100 °C for 48 h, and then filtered, washed with ethanol (95%, Kermel) to remove the excessive template. Finally, the clean and dry solid was calcined in air flow at 600 °C for 6 h to obtain SO_4^{2-}/Zr-SBA-15 materials. Pure SBA-15 sample was synthesized with TEOS, P123, H_2O, and HCl [22].

B. Characterization

The X-ray diffractometer (XRD, Shimadzu) with Cu Kα radiation (λ=0.154 nm) was used to characterize the crystallographic structure of the as-synthesized catalysts with an accelerating voltage and under a current of 40 kV and 30 mA, respectively. The morphologies of samples were observed by scanning electron microscopy (SEM, FEI Quanta 200f) operated at 30 kV. High-resolution transmission electron microscopy (HRTEM) was measured with JEOL JEM-2100F electron microscope operated at 200 kV. Surface area values S_{BET} were calculated using the BET method and pore size distribution was achieved through the BJH method assuming the cylindrical pore geometry. Total pore volume was recorded at p/p_0=0.985. The elements contents of the as-synthesized samples were determined on Thermo iCAP 6300 ICP Spectrometer. The acidity of samples was determined by ammonia temperature programmed desorption (NH$_3$-TPD). The calcined samples were out-gassed under a helium flow (25 mL/min) at 200 °C for 60 min, and then the tempera-

ture was reduced to 120 °C, and then an ammonia flow of 30 mL/min passed through the sample for 30 min. The physisorbed ammonia was removed by flowing helium at 120 °C for 30 min. The chemically adsorbed ammonia was determined by increasing the temperature up to 600 °C with a rate of 10 °C/min, afterwards maintaining this temperature for 15 min. The ammonia concentration in the effluent stream was measured through a thermal conductivity detector.

C. Transesterification reaction

Catalytic reactions were conducted in 50 mL Teflon-lined batch autoclave, equipped with a magnetic stirrer and an oil heater. The typical reaction was as follows: expired cooking oil (8.2 g), methanol (8.9 g, methanol-to-oil molar ratio of 30) and the catalyst amount (0.82 g, 10 wt% referred to oil) were placed inside the reactor and the temperature was set at 80−220 °C. The reactions were carried out for 12 h and afterwards the reactor was cooled to room temperature. The products were recovered from the reactor and mixed with methanol (25 mL), as an agent for cleaning the reactor vessel and stirrer. The final solution was filtered to recover the catalyst before removing the residual methanol in an evaporator by vacuum. In the recycling test, the recovered catalyst was calcined in air under static conditions.

Ester-rich phase (top layer) of the samples was analyzed by using a GC9890B gas chromatograph (GC) system with an AS-200 auto-injector, flame ionization detector (FID), and a DB-5ht capillary column for the determination of fatty acid methyl esters (FAME) and mono-glycerides (Mo), diglycerides (Di), and triglycerides (Tr) in the biodiesel products based on external standard method.

The conversion C of Tr, was calculated using Eq.(1).

$$C = \left(1 - \frac{C_t}{C_i}\right) \times 100\% \tag{1}$$

where t is the reaction time, C_i is the initial Tr content, and C_t is Tr content at t time.

The yield Y of FAME was calculated using Eq.(2).

$$Y = \frac{\mathrm{FAME}_t}{\mathrm{FAME}_{\mathrm{tap}}} \times 100\% \tag{2}$$

where FAME_t is FAME content at t time and $\mathrm{FAME}_{\mathrm{tap}}$ is the theoretical arithmetic products content.

III. RESULTS AND DISCUSSION

A. XRD analysis

The prepared SO$_4{}^{2-}$/Zr-SBA-15 catalysts was well-ordered mesoporous materials could be prepared. Their partial crystalline frameworks are well supported by the
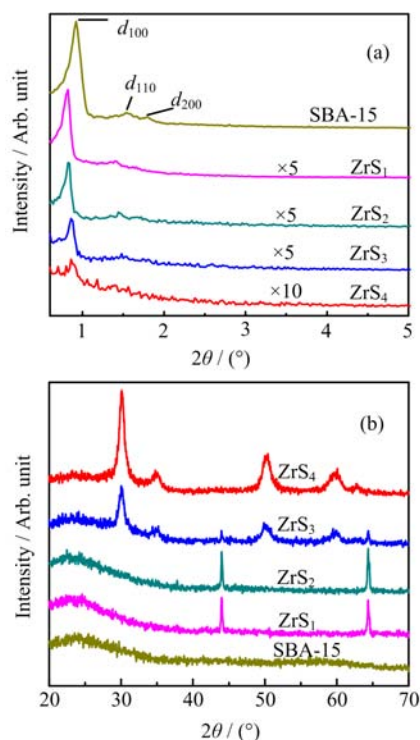
FIG. 1 XRD patterns of as-prepared catalysts with different molar ratios of 0.01, 0.02, 0.11 and 0.39 marked in ZrS$_1$, ZrS$_2$, ZrS$_3$ and ZrS$_4$, respectively. (a) Small-angle and (b) wide-angle of Zr/Si.

XRD patterns including the small-angle (Fig.1(a)) and wide-angle (Fig.1(b)) for mesoporous SO$_4{}^{2-}$/Zr-SBA-15 materials, with the results in good agreement with the previous findings [16, 17]. It is found from the Fig.1(a) that the ordering degree decreases as the zirconium content increases, but the well-ordered mesopore are still supported by small-angle peak (d_{100}) from 0.82° to 0.91°, which implies the formation of SO$_4{}^{2-}$/Zr-SBA-15 with a long-range hexagonal structure. For Fig.1(b), there exist clearly other diffraction lines (close to $2\theta = 44$° and 64°) which may be the impurity (aluminum frame substrate) peaks for ZrS$_1$ and ZrS$_2$ samples [23]. The characteristic peaks of tetragonal ZrO$_2$ phase can be observed when Zr/Si molar ratios are 0.11 (ZrS$_3$) and 0.39 (ZrS$_4$), and when the peak intensity increases with the increasing Zr/Si molar ratio. The results reveal that there exists the tetragonal ZrO$_2$ crystalline phase in the as-prepared SO$_4{}^{2-}$/Zr-SBA-15 sample.

B. SEM and TEM analysis

The SEM and TEM morphologies of ZrS$_3$ sample with Zr/Si molar ratio of 0.11 are depicted in Fig.2. It is found, that the ZrO$_2$ shows uniform distribution in the channels, and few accumulates in the channels

TABLE II Physico-chemical properties (zirconium incorporation efficiency η, interplanar spacing d_{100} calculated through the Bragg's law from XRD experiments, unit cell parameter a_0 calculated as $a_0 = 2d_{100}/\sqrt{3}$, and W_p calculated as a_0-D_p) of SO_4^{2-}/Zr-SBA-15 materials with various zirconium loading amounts.

Sample	n_{Zr}:n_{Si}	Zr/wt%	η/%	SO_4^{2-}/wt%	d_{100}/nm	a_0/nm	S_{BET}/(m^2/g)	D_p/nm	W_p/nm	V_p/(cm^3/g)
SBA-15	–	–	–		9.0	10.4	804	7.73	2.67	0.910
ZrS$_1$	0.01	1.84	5	0.17	10.7	12.4	734	7.78	4.62	0.735
ZrS$_2$	0.02	2.77	7	0.29	10.6	12.2	717	7.72	4.48	0.685
ZrS$_3$	0.11	12.44	19	1.79	10.2	11.8	707	7.67	4.13	0.636
ZrS$_4$	0.39	29.23	48	3.99	10.2	11.8	389	6.46	5.34	0.279
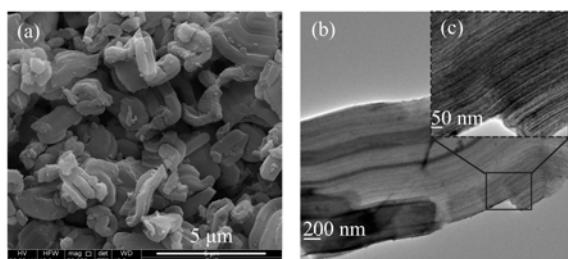
FIG. 2 (a) SEM and (b, c) TEM of ZrS$_3$ sample.

is observed from Fig.2(b)), and that the dark areas in Fig.2(b) is the distribution of ZrO$_2$. Besides, all the samples possess unambiguously the hexagonal pore structure of SBA-15 [24].

C. Physico-chemical properties

In order to determine the effect of zirconium loading on the structural properties of SO_4^{2-}/Zr-SBA-15, the zirconium loading with Zr/Si molar ratio of 0.5, 1.0, 1.5, and 2.0 was controlled, different Zr/Si molar ratio of 0.01, 0.02, 0.11, 0.39 which results in the products named as ZrS$_1$, ZrS$_2$, ZrS$_3$, ZrS$_4$. The physico-chemical properties of SO_4^{2-}/Zr-SBA-15 are listed in Table II. With the increase of zirconium content in the synthesis solution, the incorporation efficiency of zirconium amount improves. Furthermore, the calculated incorporation efficiency of ZrS$_4$ is 48%, which indicates that more zirconium species are possibly accommodated into SBA-15 structure in the saturated solution, which are also confirmed by the data of the pore-size distribution and the pore volume, as shown in Table II. All the as-prepared samples displays steep falls in the p/p_0 range from 0.40 to 0.75 (Fig.3), revealing the strong adsorption property of zirconia particle inside mesoporous channel [16], which agrees well with the calculated pore sizes distribution in Table II. Compared with ZrS$_4$ sample, other samples display narrower distribution of pore size at about 7.7 nm, and larger surface area between 707 and 734 m^2/g, both of which are rather close to those SBA-15 structure, which confirms well the ar-
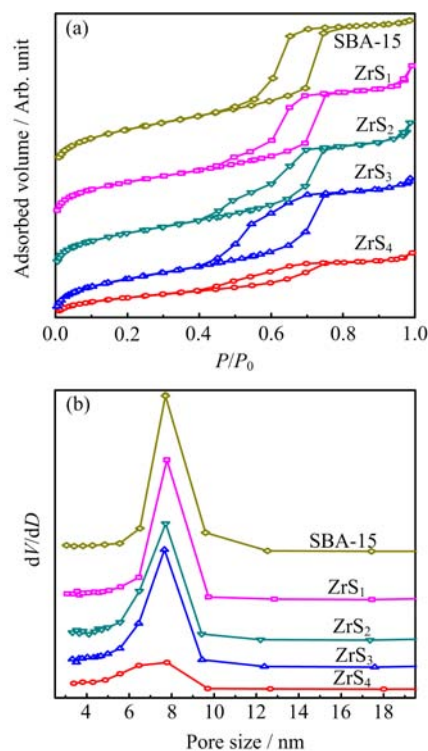
FIG. 3 (a) Nitrogen adsorption-desorption isotherms of SO_4^{2-}/Zr-SBA-15 materials with different zirconium loading amounts at 77 K, and (b) pore sizes distributions.

rangement of zirconia species onto the surface of mesoscopic channels during the calcinations of as-prepared samples.

D. NH$_3$-TPD analysis

To evaluate the effect of zirconium species on the surface of mesoporous materials, the surface acidity of as-prepared samples has been investigated by NH$_3$-TPD method. The introduction of sulfate ion could form the stable tetragonal phase of zirconia with the super acidity for sulfated zirconia [16, 25]. The NH$_3$-TPD profiles for the samples with different Zr/Si ratio (0.02−0.39)
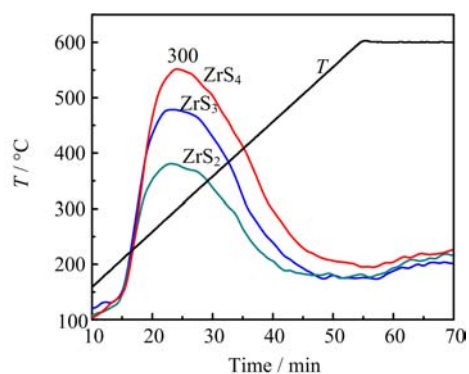
FIG. 4 NH$_3$-TPD of SO_4^{2-}/Zr-SBA-15 materials with various Zr/Si molar ratios.

FIG. 5 Reaction results for transesterification of expired cooking oil with methanol using pure silica SBA-15, SO_4^{2-}/Zr-SBA-15 and SO_4^{2-}/ZrO$_2$ as catalysts. Reaction condition: T=160 °C, t=12 h, r=30:1, 10wt% catalyst.

are displayed in Fig.4. The single desorption peaks of the samples occur at the temperature of 300 °C, and the peaks (160−540 °C) indicate the corresponding large number of acid sites, implying the intermediate and strong acid strength for SBA-15 supported zirconium functionalized materials [16, 26]. The relative acid amount can generally be estimated according to the integration area of peak in the NH$_3$-TPD curves [27]. The relative peak areas of ZrS$_2$, ZrS$_3$, and ZrS$_4$ are 135.3, 148.2, and 179.2, respectively, indicating that the order of acid amount is ZrS$_2$<ZrS$_3$<ZrS$_4$ in the SO_4^{2-}/Zr-SBA-15 materials. This could be ascribed to the higher ionicity of Zr-O bonds in zirconia-silicon materials, and be related to the strong interaction between the supported zirconia and the silica support, consequently, enhancing the Lewis acidity of metal sites [5, 16, 28].

E. Transesterification reaction

Zirconia-based material with excellent solid acid performance has been widely applied in the transesterification reaction field, exhibiting a good catalytic activity, as a kind of ideal heterogeneous acid catalyst for promising application in the transesterification reaction. However, the reaction conditions can greatly affect the conversion efficiency of waste cooling oil transesterification reaction. Therefore, a series of experiments were conducted to investigate the operational parameters, mainly involving the reaction time t, molar ratio of methanol/oil r, reaction temperature T and catalyst dosage W. In addition, the effects of Zr/Si ratios in SO_4^{2-}/Zr-SBA-15 materials on catalytic performance were also investigated.

1. Effects of Zr/Si molar ratio

The catalytic performance with methanol of zirconium silicalite catalysts in the transesterification of expired cooking oil has been initially evaluated under the
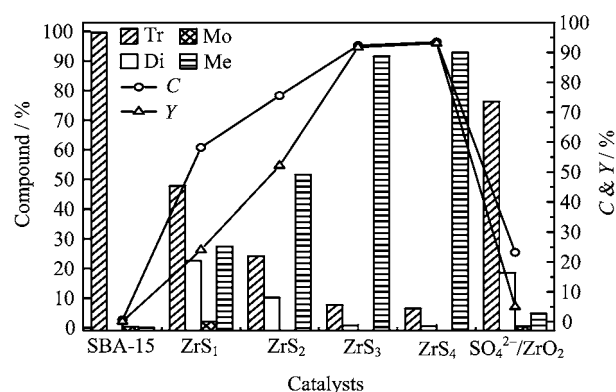
following experimental conditions: 10wt% of catalyst with respect to the oil weight, methanol/oil molar ratio of 30/1, reaction temperature of 160 °C and reaction time of 12 h. Several catalytic tests were carried out using SO_4^{2-}/Zr-SBA-15 samples with different Zr/Si molar ratios corresponding to ZrS$_n$ (n=1−4). Figure 5 displays that the conversion efficiency of triglyceride increases with the increasing zirconium loading, implying that Zr/Si ratio in SO_4^{2-}/Zr-SBA-15 materials should have an impact on the catalytic activity. It can be seen clearly that sulfated ZrO$_2$ and pure silica SBA-15 provided a rather low FAME yield of about 5% and 1%, respectively. However, the catalytic activity of SO_4^{2-}/Zr-SBA-15 materials are obviously superior to those of both sulfated ZrO$_2$ and the pure silica SBA-15, implying that the structure of SBA-15 plays an important role in the enhancement of FAME yield. A maximum conversion efficiency of 93.5% is obtained, and the FAME yield achieves 93.1% with the ZrS$_4$ sample. The activity (FAME yield of 91.7% and conversion efficiency of 92.3%) of ZrS$_3$ sample slightly decreases owing to the tetrahedrally coordinated Zr in the silicalite framework for the ZrS$_3$ sample rather than the octahedral Zr inside the surface of channel compared with those of the ZrS$_4$ sample [16, 17]. The other compounds formed in the catalytic reaction are diglycerides and mono-glycerides that only occur in the reaction for ZrS$_1$ sample. Therefore, the acid loading amount of tetrahedral zirconium species for ZrS$_3$ and ZrS$_4$ samples should be more than that of other as-prepared materials, on the basis of NH$_3$-TPD experiments.

Moreover, the catalytic activity of SO_4^{2-}/Zr-SBA-15 materials are obviously superior to that of the pure silica SBA-15 that provides a rather low FAME yield of less than 1%. The analysis of experimental results reveal that the synergistic effect of mesoporous and tetrahedral zirconium species loaded with SO_4^{2-} plays a key role in transesterification of triglyceride with alcohol. It
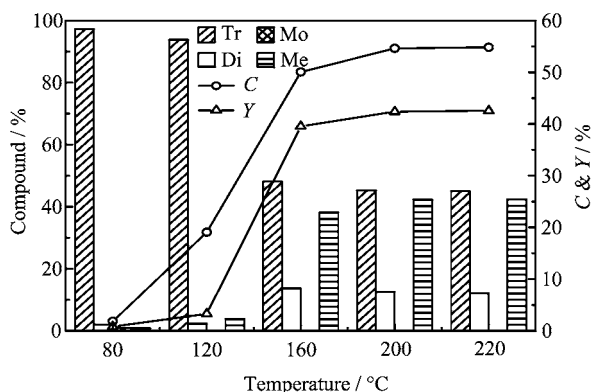
FIG. 6 Effects of reaction temperature on expired cooking oil transesterification reaction over ZrS_3 catalyst. Reaction condition: t=6 h, r=60/1, 10wt% catalyst.

FIG. 7 Effects of reaction time on transesterification of expired cooking oil with methanol over ZrS_3 catalyst. Reaction condition: T=160 °C, r=60/1, 10wt% catalyst.

is noted that the ZrS_3 and ZrS_4 catalysts are rather effective in the transesterification reaction, in good agreement with the research findings of NH_3-TPD experiments, which demonstrates that both ZrS_3 and ZrS_4 catalysts could be considered as the excellent catalytic solid acid material. On the other hand, the reaction temperature of 160 °C in our experiments is lower than the reported 200−300 °C [18, 24, 29]. As well-known, the reaction conditions can greatly affect the conversion efficiency of expired cooking oil transesterification reaction [18]. Moreover, as-prepared ZrS_3 catalyst, with the pore size of about 7.7 nm and the surface area of 707 m^2/g, could carry out the transesterification reaction of large molecule oils and fats. Therefore, a series of experiments of ZrS_3 catalyst as a representative and predominant sample were conducted to optimize the operational parameters.

2. Effects of reaction temperature

Figure 6 depicts the histogram of product compounds and point chart for triglyceride conversion using ZrS_3 sample. It is found that there exists the effect of reaction temperature on the FAME yield for the methanolysis of expired cooking oil. Although both the conversion efficiency of triglyceride and the yield of FAME are improved with the reaction temperature increasing from 80 °C to 160 °C, both of them increase slightly at the temperature between 160 and 220 °C from 50.1% to 54.8% and 39.6% to 42.6%, respectively. Thus the reaction temperature of 160 °C should be adopted for the transesterification of expired cooking oil with methanol over SO_4^{2-}/Zr-SBA-15.

3. Effects of reaction time

The effect of reaction time on the triglyceride conversion efficiency and FAME yield of biodiesel product
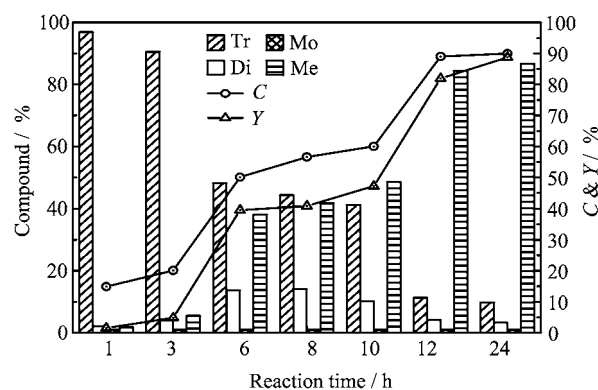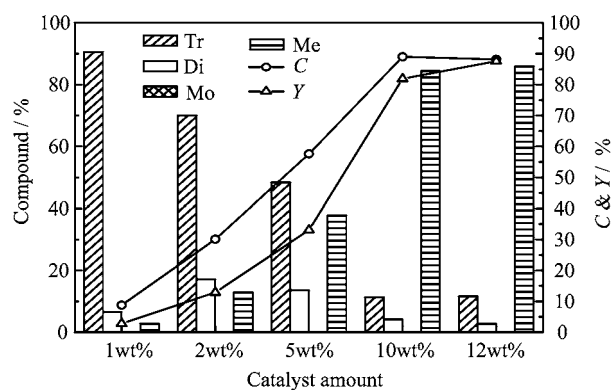
FIG. 8 Effects of catalyst dosage on the transesterification of expired cooking oil with methanol over ZrS_3 catalyst. Reaction condition: T=160 °C, t=12 h, r=60/1.

was studied from 1 h to 24 h as seen in Fig.7. With the reaction time increasing, the maximum FAME yield of 88.7% over ZrS_3 is obtained after 24 h, and the conversion efficiency of triglyceride improves gradually. Besides, the conversion efficiency increases almost up to 89% and 90%, respectively, after 12 and 24 h. In order to efficiently carry out the optimization of operation variables, a lower reaction time of 12 h should be chosen.

4. Effects of catalyst dosage

The effect of catalyst dosage on the catalytic performance for the transesterification of expired cooking oil with methanol, as shown in Fig.8, was investigated. With the SO_4^{2-}/Zr-SBA-15 (ZrS_3) catalyst dosage increasing from 1wt% to 12wt% with respect to oil weight, the FAME yield of biodiesel product was increased from 2.8% to 87.5%. Especially, the maximum triglyceride conversion of 89% is achieved at the 10wt% of catalyst dosage. Thus the 10wt% of catalyst dosage was chosen.
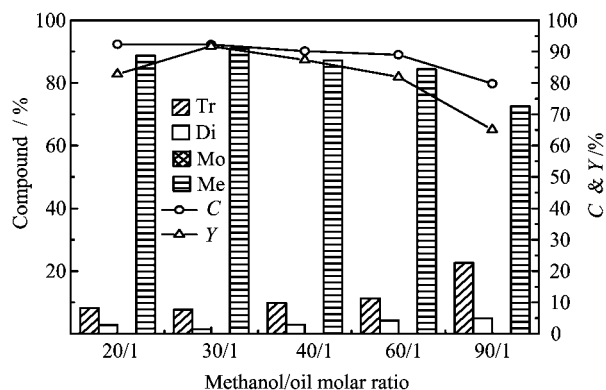
FIG. 9 Effects of the methanol/oil molar ratio on the transesterification of expired cooking oil with methanol over ZrS$_3$ catalyst. Reaction condition: T=160 °C, t=12 h, 10wt%.

FIG. 10 Effects of recycling tests on catalytic performance and the SO$_4^{2-}$ content in ZrS$_3$ (solid lines) and ZrS$_4$ (broken lines) samples. Reaction condition: T=160 °C, t=12 h, r=30:1, 10wt% catalyst.

5. Effects of methanol/oil molar ratio

The methanol/oil molar ratio has been an interesting aspect because the transesterification of triglycerides is a reversible reaction, and the excessive methanol will shift the equilibrium towards the direction of ester formation [30–32]. The transesterification of cooking oil with methanol requires three moles of methanol for each mole of oil, stoichiometrically [18, 32]. The highest conversion to methyl esters is obtained for methanol/oil molar ratio of 20/1, *i.e.*, seven times the stoichiometric molar ratio (shown in Fig.9). The highest FAME yield is obtained at the methanol/oil molar ratio of 30/1, and with the high concentration of methanol, the reaction rate can increase [33]. But the FAME yield decreases from 91.7% to 65.1% when the methanol/oil ratio is more than 30/1 as the ester is chemisorbed on the active acid sites where the carbonyl group would form a carbonium ion. Besides, the conversion efficiency of methanol to carbocation will reduce from 92.3% to 79.8%, which agrees well with the previous findings [34]. Thus, the more increment of methanol/oil molar ratio over 30/1, the lower the FAME yield, indicating the flooding of active sites with methanol molecules rather than ester molecules [33, 35].

6. Reusability of SO$_4^{2-}$/Zr-SBA-15

Note that the cyclic utilization performance of catalyst has been desirable for its practical applications, the cycling experiments of ZrS$_3$ and ZrS$_4$ samples were carried out to investigate the stability of catalyst. Under the optimal reaction conditions (reaction temperature of 160 °C, methanol/oil molar ratio of 30/1, 10wt% catalysts with respect to oil feedstock, and reaction time of 12 h), the catalytic performances of ZrS$_3$ and ZrS$_4$ were examined in the production of biodiesel, and the obtained results are plotted in Fig.10. The thermal procedure for catalyst regeneration was carried out with a
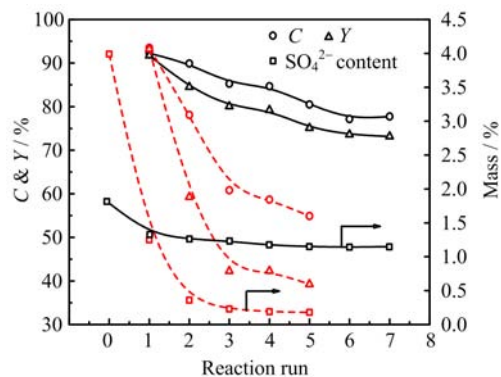
calcination step in air at 600 °C for 6 h. It is noted that the FAME yield over ZrS$_3$ reaches 91.7% and the conversion efficiency of triglyceride achieves 92.3% under the optimized conditions, while ZrS$_4$ sample has higher FAME yield than ZrS$_3$. The SO$_4^{2-}$ content decreases in the liquid mixture after the first, second or third reaction. For instance, the SO$_4^{2-}$ content of the ZrS$_3$ sample decreases from the original 1.79% to 1.23%, but that of the ZrS$_4$ sample exhibits an obvious decrease of SO$_4^{2-}$ content in the liquid mixture after the first, second or third reaction in that the SO$_4^{2-}$ content reduces from the original 3.99% to 0.23%. Table III shows catalyst characteristics comparison between reaction before and after. The results further reveal that the main reason of "catalyst deactivation" is due to the loss of SO$_4^{2-}$ of catalyst surface into the reaction system, and parts of that existed steadily in the catalyst framework keep the excellent catalytic activity and stability for ZrS$_3$ sample. In addition, Melero *et al.* [36] also suggested that the major cause of deactivating behavior may contribute to the hindered access of the reactants for the catalytic acid sites because of the adsorption of these substances onto the surface of the silica matrix as well as on to the catalytic acid sites. Nevertheless, our catalysts have been demonstrated to be highly resistant against poisoning even being reused more than twice or thrice. More importantly, it is interesting and valuable to investigate the modification of the catalyst about the heat treatment at 600 °C between each catalytic run in the future.

Furthermore, there is no obvious change in the activity of ZrS$_3$ even after six regenerations, which should be ascribed to its higher area of mesoporous framework and surface acidity on the basis of the above mentioned analysis results. However, the FAME yield over ZrS$_4$ decreases to 39.3% after four times recycles, which may be resulted from the loss of its surface acidity. Moreover, the decrease in activity of ZrS$_4$ was derived from the loss of active center of catalyst in the filtration pro-

TABLE III catalyst characteristics comparison before and after reaction.

Run	$C/\%$	$Y/\%$	$SO_4^{2-}/\text{wt}\%$	$S_{BET}/(\text{m}^2/\text{g})$	D_p/nm	$V_p/(\text{cm}^3/\text{g})$	Peak areas in NH_3-TPD
ZrS_3			1.79	707	7.67	0.636	148.2
1st	92.2363	91.7525	1.34	715	7.69	0.667	143.3
2nd	89.8952	84.4950	1.26	723	7.69	0.670	139.7
3rd	85.2606	80.0551	1.23	728	7.68	0.681	138.5
4th	84.6744	79.2303	1.17	727	7.70	0.679	136.9
5th	80.4825	75.0895	1.15	726	7.69	0.682	135.8
6th	77.1394	73.5854	1.14	731	7.70	0.683	135.5
7th	77.7299	73.1590	1.15	729	7.71	0.685	135.7

TABLE IV Comparison of catalyst comprehensive performance. y: repeatability FAME yield.

Catalyst	Feedstock	Zr/Si	S/Zr	$T/°C$	$W/\text{wt}\%$	t/h	$C/\%$	$Y/\%$	$y/\%$	Run
SZr-SBA-15[a] [37]	$ZrOCl_2 \cdot 8H_2O$	1/7.1	0.63	60	4.5	12	72.9	28.6		
Na/Zr-SBA-15[a] [38]	$ZrOCl_2 \cdot 8H_2O$	1/27.6		70	12(15wt%Na)	6		99	85%	Three times
Zr-SBA-15[b] [5]	Cp_2ZrCl_2	1/10		200	10	3		72	70%	Four times
SZr-SBA-15[a] [21]	$Zr(OC_3H_7)_4$	1/2.5	0.11	200	5	10	>95	>85%		Five times
Zr-SBA-15[b] [18]	Cp_2ZrCl_2	1/10		209	12.45	6		92	60%	Four times
Zr-SBA-15[c] [39]	Cp_2ZrCl_2	1/2.6		210		0.5		96		
SO_4^{2-}/Zr-SBA-15[d]	$Zr(NO_3)_4$	1/9	0.14	160	10	12	92.3	91.7	74±1%	Seven times

[a] Impregnated after synthesis.
[b] One pot.
[c] Grafting after synthesis.
[d] In this work.

cess for the cycle utilization, but the catalyst structure has not been changed in the catalytic reaction. Our experiment results demonstrate that ZrS_3 sample should possess the excellent catalytic activity and stability, and became as well a kind of potential industrial catalyst applied in biodiesel production by transesterification of expired cooking oil with methanol.

F. Comparison of catalyst comprehensive performance

Table IV shows the performances of different Zr-SBA-15 materials obtained from different feedstocks and synthesis methods. It is obvious that the reported as-prepared samples [37, 38] present the lowest reaction temperature, however, the triglyceride conversion efficiency and FAME yield are lower than those of other catalysts [37], and although it shows the highest FAME yield, the feedstock ($ZrOCl_2 \cdot 8H_2O$) is difficult to be obtained and the synthesis method is relative complicated compared with one-step process [38]. In this study, the Zr-SBA-15 materials synthesized by one-step method from $Zr(NO_3)_4$, are cheap and easy to be acquired. More importantly, the Zr-SBA-15 has high triglyceride conversion efficiency (92.3%), FAME yield (91.7%), and reusability (7 times, FAME yield (74±1)%) at a mild reaction temperature (160 °C). The excellent compre-

hensive performance suggests that Zr-SBA-15 will have competitive advantage in biodiesel production from expired cooking oil.

IV. CONCLUSION

In this work, SO_4^{2-}/Zr-SBA-15 materials were successfully synthesized by one-step process using anhydrous zirconium nitrate as the zirconium resource, and their reaction behaviors were studied in biodiesel production from waste cooking oil with methanol. The results indicate that one-step synthesis allows the preparation of Zr-base functionalized materials with a high amount of metal loading, and preserving the high mesoscopic ordering typical from SBA-15 materials. The reaction parameters, such as reaction temperature, catalyst loading, methanol/oil molar ratio and reaction time, remarkably affect the reaction rate for biodiesel production from expired cooking oil. The as-prepared SO_4^{2-}/Zr-SBA-15 samples present the excellent catalytic activity in the transesterification of expired cooking oil with methanol, under the optimized reaction conditions: 10wt% of catalyst with respect to oil weight, methanol/oil molar ratio of 30/1, reaction temperature of 160 °C, and reaction time of 12 h. The obtained triglyceride conversion efficiency and FAME

yield achieve 92.2% and 91.8%, respectively. Furthermore, SO_4^{2-}/Zr-SBA-15 (ZrS$_3$) sample reveals the higher area of mesoporous framework and surface acidity by binding the zirconium species onto the surface of SBA-15 material, obtaining the excellent stability and reusability, so that SO_4^{2-}/Zr-SBA-15 (ZrS$_3$) catalyst still remains the high FAME yield of (74±1)% after seven reaction runs, and it could become a kind of potential industrial catalyst to be applied in biodiesel production by transesterification of waste cooking oil with methanol.

V. ACKNOWLEDGMENTS

[1] K. K. Höinghaus, P. Oßwald, T. A. Cool, T. Kasper, N. Hansen, F. Qi, C. K. Westbrook, and P. R. Westmoreland, Angew. Chem. Int. Ed. **49**, 3572 (2010).

[2] A. T. Kiakalaieh, N. A. S. Amin, and H. Mazaheri, Appl. Energy **104**, 683 (2013).

[3] E. A. Torres, G. S. Cerqueira, T. M. Ferrer, C. M. Quintella, M. Raboni, V. Torretta, and G. Urbini, Waste Manage. **33**, 2670 (2013).

[4] Z. Yaakob, M. Mohammad, M. Alherbawi, Z. Alam, and K. Sopian, Renew. Sust. Rev. **18**, 184 (2013).

[5] J. Iglesias, J. A. Melero, L. F. Bautista, G. Morales, R. S. Vázquez, M. T. Andreola, and A. L. Fernández, Catal. Today **167**, 46 (2011).

[6] R. Sheikh, M. S. Choi, J. S. Im, and Y. H. Park, J. Ind. Eng. Chem. **19**, 1413 (2013).

[7] Z. X. Du, Z. Tang, H. J. Wang, J. L. Zeng, Y. F. Chen, and E. Z. Min, Chin. J. Catal. **34**, 101 (2013).

[8] Z. Man, Y. A. Elsheikh, M. A. Bustam, S. Yusup, M. A. Mutalib, and N. A Muhammad, Ind. Crop. Prod. **41**, 144 (2013).

[9] P. T. Vasudevan and M. Briggs, J. Ind. Microbiol. Biotechnol. **35**, 421 (2008).

[10] S. G. Chopade, K. Kulkarni, A. Kulkarni, and N. S. Topare, Acta. Chim. Pharm. Indica. **2**, 8 (2012).

[11] C. S. Cordeiro, F. Silva, F. Wypych, and L. P. Ramos, Quím. Nova. **34**, 477 (2011).

[12] A. Baig and F. T. Ng, Energy Fuels **24**, 4712 (2010).

[13] R. S. Vázquez, C. Pirez, J. Iglesias, K. Wilson, A. F. Lee, and J. A. Melero, ChemCatChem **5**, 994 (2013).

[14] J. A. Melero, J. Iglesias, and G. Morales, Green Chem. **11**, 1285 (2009).

[15] K. Arata, Green Chem. **11**, 1719 (2009).

[16] R. F. Li, F. Yu, F. X. Li, M. M. Zhou, B. S. Xu, and K. C. Xie, J. Solid State Chem. **182**, 991 (2009).

[17] F. X. Li, F. Yu, Y. L. Li, R. F. Li, and K. C. Xie, Micropor. Mesopor. Mater. **101**, 250 (2007).

[18] J. Melero, L. Bautista, J. Iglesias, G. Morales, and R. S. Vázquez, Catal. Today **195**, 44 (2012).

[19] Y. Wang, J. H. Ma, D. Liang, M. M. Zhou, F. X. Li, and R. F. Li, J. Mater. Sci. **44**, 6736 (2009).

[20] M. D. Gracia, A. M. Balu, J. M. Campelo, R. Luque, J. M. Marinas, and A. A. Romero, Appl. Catal. A **371**, 85 (2009).

[21] W. Thitsartarn and S. Kawi, Ind. Eng. Chem. Res. **50**, 7857 (2011).

[22] D. Y. Zhao, J. L. Feng, and Q. S. Huo, Science **279**, 548 (1998).

[23] A. M. Esawi, K. Morsi, A. Sayed, A. A. Gawad, and P. Borah, Mater. Sci. Eng. A **508**, 167 (2009).

[24] D. Y. Zhao, J. Y. Sun, Q. Z. Li, and G. D. Stucky, Chem. Mater. **12**, 275 (2000).

[25] G. D. Yadav and A. D. Murkute, Adv. Synth. Catal. **346**, 389 (2004).

[26] O. Rahmanpour, A. Shariati, and M. K. Nikou, Int. J. Chem. Eng. Appl. **3**, 125 (2012).

[27] J. J. Zheng, J. H. Ma, Y. Wang, Y. D. Bai, X. W. Zhang, and R. F. Li, Catal. Lett. **130**, 672 (2009).

[28] D. Nedumaran and A. Pandurangan, Micropor. Mesopor. Mater. **169**, 25 (2013).

[29] M. J. Li, Z. C. Feng, P. L. Ying, Q. Xin, and C. Li, Phys. Chem. Chem. Phys. **5**, 5326 (2003).

[30] A. P. Vyas, J. L. Verma, and N. Subrahmanyam, Adv. Chem. Eng. Sci. **1**, 45 (2011).

[31] K. Jacobson, R. Gopinath, L. C. Meher, and A. K. Dalai, Appl. Catal. B **85**, 86 (2008).

[32] J. L. Zhang, Z. T. Zhao, Y. Qiao, H. Lin, X. Y. Pang, Q. R. Bai, and R. F. Li, China J. Chem. Ind. Eng. **63**, 1684 (2012).

[33] A. J. López, I. J. Morales, J. S. González, and P. M. Torres, J. Mol. Catal. A **335**, 205 (2011).

[34] J. A. Melero, L. F. Bautista, G. Morales, J. Iglesias, and R. S. Vázquez, Chem. Eng. J. **161**, 323 (2010).

[35] W. Y. Lou, J. Cai, Z. Q. Duan, and M. H. Zong, China J. Catal. **32**, 1755 (2011).

[36] J. A. Melero, L. F. Bautista, J. Iglesias, G. Morales, R. S. Vázquez, K. Wilson, and A. F. Lee, Appl. Catal. A **488**, 111 (2014).

[37] Y. Du, S. Liu, Y. Zhang, F. Nawaz, Y. Ji, and F. S. Xiao, Micropor. Mesopor. Mater. **121**, 185 (2009).

[38] W. K. Chen, H. H. Tseng, M. C. Wei, E. C. Su, and I. C. Chiu, Int. J. Hydrogen Energ. **39**, 19555 (2014).

[39] J. A. Melero, L. F. Bautista, J. Iglesias, G. Morales, and R. S. Vázquez, Appl. Catal. B **145**, 197 (2014).